LUND UNIVERSITY
Faculty of Medicine

LUP

Lund University Publications
Institutional Repository of Lund University

This is an author produced version of a paper published in Cephalalgia : an international journal of headache. This paper has been peer-reviewed but does not include the final publisher proof-corrections or journal pagination.

Citation for the published paper:
Y Liu, Jonas Broman, Mengliang Zhang, Lars Edvinsson

"Brainstem and thalamic projections from a craniovascular sensory nervous centre in the rostral cervical spinal dorsal horn of rats."
Cephalalgia : an international journal of headache, 2009, Issue: Feb 25

http://dx.doi.org/10.1111/j.1468-2982.2008.01829.x

Access to the published version may require journal subscription.

Published with permission from: Blackwell

Brainstem and thalamic projections from a craniovascular sensory nervous center in the rostral cervical spinal dorsal horn of rats

Yi Liu[1], Jonas Broman[2,3], Mengliang Zhang[4], Lars Edvinsson[1]

[1]Department of Clinical Science, Experimental Vascular Research, Lund University, S-221 85 Lund, Sweden

[2]Department of Experimental Medical Science, Division of Neuroscience, Lund University, S-221 84 Lund, Sweden

[3]Department of Neuroscience, Karolinska Institute, S-171 77 Stockholm, Sweden

[4]Department of Neuroscience and Pharmacology, the Panum Institute, Copenhagen University, DK-2200 Copenhagen, Denmark

Corresponding author:

Yi Liu, MD, PhD., Department of Clinical Science, Experimental Vascular Research, BMC A13, Lund University, S-221 85 Lund, Sweden

Tel: + 46 46 2220603

Fax: + 46 46 2220616

Email: liuyi0724@hotmail.com

Total number of text: 29

Number of table: 1

Number of figures: 4

Abstract

To examine the ascending projections from the headache-related trigeminocervical complex in rats, we injected biotinylated dextran amine (BDA) into the ventrolateral dorsal horn of segments C1 and C2, a region previously demonstrated to receive input from sensory nerves in cranial blood vessels. Following injections into laminae I-II, BDA-labeled terminations were found bilaterally in several nuclei in the pons and the midbrain, including the pontine reticular nucleus, the parabrachial nuclei, the cuneiform nucleus, and the periaqueductal gray. In the diencephalon, terminations were confined to the contralateral side and evident foremost in the posterior nuclear group, especially its triangular part, and in the ventral posteromedial nucleus. Following injections extending through laminae I-IV, anterograde labeling was more extensive. Some of the above regions are likely to be involved in the central processing of noxious signals of craniovascular origin and therefore putatively involved in mechanisms associated with primary headaches.

Key words: cranial vessel; anterograde tracing; ascending projection; nociception; headache

Abbreviations

I-V	laminae I-V of spinal grey matter
3	oculomotor nucleus
7n	facial nerve or its root
APT	anterior pretectal nucleus
Aq	aqueduct
BDA	biotinylated dextran amine
CIC	central nucleus of the inferior colliculus
CnF	cuneiform nucleus
Cp	cerebral peduncle basal part
DCIC	dorsal cortex of the inferior colliculus
DpG	deep gray layer of the superior colliculus
DpMe	deep mesencephalic nucleus
DpWh	deep white layer of the superior colliculus
ECIC	external cortex of the inferior colliculus
fr	fasciculus retroflexus
IMD	intermediodorsal thalamic nucleus
InCo	intercollicular nucleus
InG	intermediate gray layer of the superior colliculus
InWh	intermediate white layer of the superior colliculus
LCN	lateral cervical nucleus
Ll	lateral lemniscus
LPB	lateral parabrachial nucleus
ml	medial lemniscus
Mo5	motor trigeminal nucleus

MPB	medial parabrachial nucleus
Op	optic nerve layer of the superior colliculus
opt	optic tract
PAG	periaqueductal gray
PB	parabrachial nucleus
PIL	posterior intralaminar thalamic nucleus
Pli	posterior limitans thalamic nucleus
PnC	pontine reticular nucleus, caudal part
Po	posterior thalamic nuclear group
PoT	posterior thalamic nuclear group, triangular part
PR	prerubral field
Pr5DM	principal sensory trigeminal nucleus, dorsomedial part
Pr5VL	principal sensory trigeminal nucleus, ventrolateral part
PrC	precommissural nucleus
R	red nucleus
REth	retroethmoid nucleus
RRF	retrorubral field
s5	sensory root of the trigeminal nerve
SG	suprageniculate thalamic nucleus
Sm	submedial nucleus
SN	substantia nigra
sox	suproptic decussation
Sp5C	spinal trigeminal nucleus, caudal part
Sp5O	spinal trigeminal nucleus, oral part
SPF	subparafascicular thalamic nucleus

SubC	subcoeruleus nucleus
VM	ventromedial thalamic nucleus
VPL	ventral posterolateral thalamic nucleus
VPM	ventral posteromedial thalamic nucleus
ZI	zona incerta

Introduction

The expression of pain in primary headaches is associated with activity in intracranial perivascular sensory nerve fibers, which originate in the trigeminal ganglion and project to the trigeminocervical complex in the brainstem. To understand the mechanisms of head pain in the pathogenesis of headaches, it is important to identify the CNS regions that process nociceptive information from the trigeminovascular system (1). Accumulating evidence demonstrate that a major central target of some of the cranial perivascular nerves locate in a ventrolateral region of the dorsal horn extending from segment C3 rostrally into the caudal part of the spinal trigeminal nucleus (Sp5C) (2-9). This region, referred to as the "trigeminocervical complex", is likely to be involved in headaches (6). We have previously demonstrated, using transganglionic tract tracing, that sensory nerve fibers in the superficial temporal artery, the superior sagittal sinus and the middle meningeal artery, all terminate in this region (7-9). Thin caliber primary afferent fibers (labeled with wheat germ agglutinin-horseradish peroxidase conjugate; WGA-HRP) were found to terminate in laminae I-II, whereas larger caliber fibers (labeled with cholera toxin subunit B; CTb) terminated in laminae III-IV.

Evidence from animal experiments indicates that many regions in the brainstem and diencephalon may be involved in the pathophysiology of migraine (10-13). Using positron emission tomography (PET) and functional magnetic resonance imaging (fMRI), several regions in the human brainstem, thalamus, hypothalamus and cerebral cortex have been observed to increase their activities during somatic nociceptive stimuli and in migraine attacks (14-17). It is unclear to what extent such activities depend on direct input from trigeminocervical neurons relaying nociceptive signals from cranial blood vessels. Therefore, to further understand the neural mechanisms behind primary headaches, it is important to know where neurons in this headache-related trigeminocervical complex project in the brainstem and

in the thalamus. Such knowledge may also be of value in developing novel strategies to relieve headaches.

Ascending projections from the spinal dorsal horn have been extensively examined in different species using the high-resolution anterograde tracers *Phaseolus vulgaris* leucoagglutinin (PHA-L) and/or biotinylated dextran amine (BDA) (e.g., 18-24). However, none of these studies have specifically addressed the ascending projections from the cranial blood vessel-receptive area in the rostral cervical spinal dorsal horn. We therefore in this study traced the brainstem and thalamic projections from this area, using BDA as anterograde tracer.

Methods

Surgery and tracer injections

The experimental procedures was reviewed and approved in advance by the Animal Care and Use Committee of Malmö/Lund. Thirty adult male Sprague-Dawley rats weighing 250-400 g were used in this study. The rats were deeply anesthetized with chloral hydrate (300 mg/kg, i.p.) and mounted in a stereotaxic frame. A sagittal incision was made on the back of the neck and a laminectomy was performed to gain access to the C1 and C2 segments of the spinal cord. A glass micropipette (outside tip diameter 25-40 μm), filled with 10% BDA (Molecular Probes, Eugene, Oregon, USA), was positioned about 1.6 mm lateral to the midline of segments C1 or C2 and with an angle of 10-15º towards the sagittal plane. The tip of the micropipette was carefully inserted through a small opening of the dura mater into the ventrolateral part of dorsal horn, aiming at either the superficial (laminae I-II) or the deeper layers (laminae III-IV). The BDA was injected iontophoretically using an interrupted current (5 μA, 7 s on / 7 s off) for about 20-25 minutes. Only one injection was made in each rat and all injections were placed on the right side. After a postoperative survival period of one to three weeks, the rats were deeply anesthetized with sodium pentobarbital and terminated by transcardial perfusion. Following a

rinse with 500 ml of 0.1 M phosphate-buffered saline (PBS), the rats were fixed by perfusion with 700 ml of 4% paraformaldehyde in PBS at room temperature for 30 min. The brain and the rostral part of the spinal cord were removed and placed in fixative overnight at 4ºC. The tissues were then put into PBS containing 30% sucrose for 1-2 days.

Tissue processing

The brain and the rostral spinal cord containing the injections site were blocked and cut coronally into 40 µm thick sections on a freezing microtome. Four sets of sections were collected. One set of sections were mounted on slides and stained with thionin (Merck, Darmstadt, Germany). To visualize BDA labeling, one adjacent set of sections were rinsed in PBS with 0.3% Triton (PBS-T) and then incubated in ABC Elite solution (Vector Laboratories, Burlingam USA; one drop of A plus one drop of B in 5 ml of PBS-T) for four hours at room temperature or overnight at 4ºC. After several rinses in 0.01M PBS (PH 7.5), the sections were processed with the chromogen Vector SG (Vector Laboratories, Burlingame, USA; three drops each of the chromogen and the H_2O_2 solution in 5 ml 0.01M PBS) for 10-15 minutes until a Golgi-like black staining of fibers and terminals appeared. The sections were then rinsed and mounted on slides. The sections containing the injection sites were counterstained with neutral red to reveal the cytoarchitecture of the spinal cord. The sections were dried, cleared in xylene and cover-slipped with DPX (VWR International AB, Stockholm, Sweden).

Data analysis

Anterograde labeling in the brain and spinal cord sections were examined in a light microscope (Nikon Optiphot-2) and photographed with a Q-Imaging Micropublisher 5.0 digital camera. The photomicrographs were processed in Adobe Photoshop (version 9.0) to enhance the visibility of labeled profiles. Every third or fourth section containing BDA-labeled terminal-

like varicosities was plotted using a computer-assisted plotting system (MD2 & MDplot system, Minnesota Datametrics Corp., Shoreview, MN, USA) connected to the microscope. The resulting plots were compared with the adjacent thionin-stained sections to define the cytoarchitectonic borders of different nuclei. The atlas of Paxinos and Watson (25) was used as a reference for terminology and delineation of nuclei.

Results

Injection sites

Altogether thirty rats were subjected to BDA injections. Of these, seven rats displayed BDA injections that were confined to either laminae I-II (n=3) or laminae I-IV (n=4) in the lateral part of the C1 or C2 dorsal horn (Fig. 1 A-D). Two additional rats had injections in laminae I-IV that also extended slightly into the adjacent lateral cervical nucleus (LCN; Fig. 1 E). The remaining rats had injections extending outside of these regions and the ascending projections labeled in these rats were therefore not analyzed in detail.

Anterograde labeling in the brainstem and thalamus

The focus of the present study was to search for putative vascular sensory centers in the brainstem and the thalamus. In the medulla, terminal labeling was evident only in the ipsilateral trigeminal nuclear complex. Because we cannot exclude that at least a proportion of this labeling resulted from uptake of the tracer in trigeminal tract fibers passing or terminating within the injection site, this labeling was not analyzed in detail.

Table 1 lists the distribution and relative abundance of BDA-labeled varicosities in the pons, the midbrain and the thalamus for all examined cases. The density and distribution of terminal labeling differed between the different cases. The cases with an injection including

laminae I-IV generally showed more abundant labeling than those with an injection limited to laminae I-II (see also Fig. 2).

BDA injections in laminae I-II. The group with injections confined to laminae I-II includes three rats (rats 26, 56 and 58; Fig. 1A and C). In rat 26, the BDA injection was located in the C1 segment, included the lateral part of lamina I-II and had a rostrocaudal extension of about 1000 μm (Fig. 1A). Anterograde labeling in this case was relatively abundant and BDA-labeled terminal-like varicosities were evident in several nuclei in the pons, the midbrain and the thalamus (Fig. 2A). In the pons, relatively dense terminal labeling was detected in lateral parabrachial nucleus (LPB), whereas labeling was sparser in its medial part (MPB) (Fig. 3A). Terminal labeling was also detected in the caudal part of pontine reticular nucleus (PnC) and in the subcoeruleus nucleus (SubC). In the midbrain, moderate labeling was detected in the cuneiform nucleus (CnF), in the lateral and ventrolateral parts of the periaqueductal gray (PAG), in the intermediate gray layer of the superior colliculus (InG) (Fig. 3B-D), and in the deep mesencephalic nucleus (DpMe). Sparse labeling was evident in the anterior pretectal nucleus (APT). In the thalamus, dense labeling was detected in the triangular part of posterior nuclear group (PoT) and in the ventral posteromedial nucleus (VPM) (Fig4. A, B). Moderate labeling was seen in the posterior nuclear group (Po) and in the ventromedial nucleus (VM). Except for in the DpMe, labeling in the pons and in the midbrain was bilateral, whereas labeling in the DpMe and in the thalamus was confined to the side contralateral to the BDA injection.

The BDA injection sites in rats 56 and 58 located in the rostral part of C2 and were smaller than that in rat 26. The injections included a small part of laminae I-II in the lateral part of dorsal horn and had a rostrocaudal extension of about 600 μm (Fig. 1 C). Terminal labeling in the pons and in the midbrain of these two cases was generally sparser than in rat 26, but had

a similar distribution. In the thalamus of rat 56, anterograde labeling was only detected in the PoT, whereas in rat 58 terminal labeling was evident also in the VPM (Table 1).

BDA injections in laminae I-IV. The group with injections extending through laminae I-IV includes four rats (rats 51, 55, 85 and 87; Fig. 1B and D). Rats 51, 55 and 87 had closely similar injection sites. They all located in the ventrolateral part of the dorsal horn and formed a narrow strip across laminae I-IV, with a center in lamina III (rat 55) or laminae III-IV (rats 51 and 87). The rostrocaudal spread of the injections in these three cases varied between 800 and 1200 μm. The injection site in rat 85 located in the lateralmost part of the dorsal horn but did not spread into the adjacent white matter. It was centered in lamina III and extended rostrocaudally for about 1500 μm. Rats 51 and 55 displayed closely similar anterograde labeling patterns in the brainstem and thalamus, labeling that was less abundant and comprised fewer nuclei than in rats 85 and 87. The nuclei in the brainstem and the thalamus that contained anterograde labeling in both rats 51 and 55 were the PnC, the LPB, the CnF, the DpMe, the APT, the PoT and the posterior intralaminar thalamic nucleus (PIL) (Table 1). Besides those nuclei, the SubC and the MPB in the pons and the InG in the midbrain were labeled in rat 55 but not in rat 51, whereas the PAG in the midbrain and the suprageniculate nucleus (SG) in the thalamus were labeled in rat 51 but not in rat 55. In rat 51, labeling was only detected on the contralateral side. In rat 55, except for the LPB, the MPB and the SubC, which all showed bilateral labeling, anterograde labeling was confined to the contralateral side. Except for a few nuclei where anterograde labeling was relatively dense, like in the LPB of rat 55, most nuclei contained sparse to moderate labeling.

Rats 85 and 87 showed closely similar anterograde labeling patterns. All nuclei in the brainstem that were labeled in rats 51 and 55 were also labeled in rats 85 and 87, in which brainstem labeling was mostly bilateral. In addition, sparse to moderate labeling was detected in the deep gray layer of the superior colliculus (DpG). In the thalamus of rats 85 and 87

anterograde labeling was confined to the contralateral side but was more extensive than in rats 51 and 55. In addition to the PoT and the Po, the VPM, the VM, the SG and the PIL, also the ventral posterolateral nucleus (VPL) contained anterograde labeling in rats 85 and 87 (Fig. 4C). The density of terminal-like varicosities was moderate in most thalamic nuclei, although a few, like the VPL, displayed a high density of labeled terminations.

BDA injections in laminae I-IV that extended into the LCN. Two rats had injections forming wedge-shaped strips across lateral laminae I-IV in the caudal C1 (rat 27) or rostral C2 (rat 29), injections that also extended into the adjacent LCN (Fig. 1E). The rostrocaudal extent of the injections was 1000 μm and 1200 μm, respectively. As seen in Table 1, the overall labeling patterns and densities of terminal-like varicosities in these rats were similar to those in rats 85 and 87, except for some additional labeling evident only in rats 27 and 29. The nuclei containing labeled varicosities in the pons and the midbrain of rats 27 and 29 include the SubC, the PnC, the LPB, the MPB, the PAG, the CnF, the DpMe and the InG. The DpG was labeled only in rat 29. The labeling was mostly bilateral. The central nucleus (CIC) and the external cortex of the inferior colliculus (ECIC) were found to contain anterograde labeling (confined to the contralateral side) only in rats 27 and 29. In the thalamus, anterograde labeling had distributions similar to those in rats 85 and 87 and was confined to the contralateral side.

Summary. Although the distribution and density of terminal-like varicosities differed between the different injection groups and in some extent also within groups, some common characteristics could still be extracted. For example, in the pons and midbrain, the labeling was generally present bilaterally although some nuclei showed more prominent labeling on the contralateral side. In the thalamus, terminal labeling was confined to the contralateral side in all cases. Overall, the labeling patterns in the pons and the midbrain were similar in the cases with an injection that was limited to laminae I-II and in those where the injection extended through laminae I-IV. The PnC, the LPB, and the MPB in the pons, the CnF, the PAG, the

DpMe and the APT in the midbrain, contained moderate to dense terminal-like labeling irrespective of the injections including laminae I-II or laminae I-IV. In the thalamus, anterograde labeling was more extensive when tracer injections in addition to laminae I-II also included laminae III-IV. Thus, the PIL, the VPL and the SG contained labeling only when the injections extended into laminae III-IV. The PoT, the Po and the VPM were labeled after injections into both laminae I-II and laminae I-IV. The CIC and the ECIC displayed anterograde labeling only when injections comprising laminae I-IV also involved the LCN (rats 27 and 29). Otherwise, the distributions of anterograde labeling in rats 27 and 29 were similar to those in rats 85 and 87, i.e., the two rats with the most extensive labeling following BDA injections comprising laminae I-IV but not the LCN.

Discussion

To our knowledge, this is the first study that examines ascending projections from the ventrolateral part of the C1/C2 dorsal horn, an area that has been demonstrated to receive primary afferent terminations from sensory nerves in several cranial blood vessels (2, 3, 7-9). A large number of nuclei in the brainstem and the thalamus receive projections from this area, including the lateral and medial parts of parabrachial nucleus (PB), the CnF, the PAG, the DpMe, the InG and the APT in the brainstem, the Po, the PoT and the VPM in the thalamus. Although it appears unlikely that all of these nuclei are directly involved in the expression of primary headaches, at least some of them might play a role in the transmission and/or modulation of nociceptive signals from nerves in the cranial vasculature. The results may in addition provide a guide for further physiological and pathophysiological studies to explore the mechanism of headache.

Methodological considerations

Many different tracers have been used for anterograde labeling of nerve fibers in the CNS, including WGA-HRP, PHA-L, BDA and different fluorophores (22, 24, 26, 27). To obtain largely selective anterograde labeling, BDA and PHA-L are commonly used. There are several common features for these two tracers. First, both of them can be injected iontophoretically to produce small and well-defined injections sites. Second, anterogradely labeled structures display a "Golgi-like" appearance, making it easier to differentiate nerve fibers and terminal boutons. In comparison with PHA-L, BDA labeling usually has a lower failure rate and the staining procedure for BDA is simpler (28). We therefore decided to use BDA in the present work. An obvious drawback of the small injections obtained with BDA, as well as PHA-L, is that relatively few neurons will absorb the tracer, resulting in relatively sparse anterograde labeling especially if the number of projection neurons in the injected area is already small. To compensate for this, several injections may be placed in the area of interest. However, this would also increase the risk of contaminating areas outside of that to be labeled (e.g., laminae I-II), and we therefore choose to make a single injection in each rat. Because of this, the anterograde labeling obtained in the present experiments most likely underestimates the density of ascending projections from the ventrolateral dorsal horn at C1/C2.

We injected BDA into the ventrolateral part of the C1 or C2 dorsal horn as this region was found to be a primary target of afferent fibers in several cranial blood vessels (7-9). However, this does not mean that all neurons within this area are involved in headaches. Some neurons are likely to receive and convey inputs primarily or exclusively from different types of low-threshold receptors (for review, see 29). Neurons in the spinal and trigeminal dorsal horns have different physiological properties, some responding to low-threshold inputs, others to high-threshold inputs and still others to both (wide-dynamic-range neurons) (30). Thus, the terminations detected in this study are likely to be involved in a variety of sensory and motor functions associated with the ventrolateral C1/C2 dorsal horn.

In two rats with BDA injections in laminae I-IV, the injections also extended into the LCN. The only nuclei found to contain anterograde labeling in these rats but not in rats with injections confined to laminae I-IV, were the CIC and the ECIC in the midbrain. It therefore appears likely the anterogradely labeled fibers in these nuclei originate in the LCN. Ascending projections from the LCN has mostly been investigated in cats and other carnivores (see e.g., 27, 31, 32). However, the organization of ascending LCN projections in rats appears to be basically similar to those in carnivores, including abundant termination in the intercollicular area and the deep layers of the superior colliculus in the midbrain, and in the VPL of the thalamus (33). Anterograde labeling in these regions were also detected in this study and it appears likely that at least a proportion of such labeling in rats 27 and 29 originates in the LCN.

The glass capillaries used to inject BDA was inserted into the dorsal horn through the thin rim of white matter dorsal to the ventrolateral dorsal horn. It is therefore possible that primary afferent fibers in the trigeminal tract descending to this level may have taken up the tracer. Thus, labeling in the ipsilateral nuclei of the spinal trigeminal tract may have included labeling of spinal trigeminal tract fibers and were therefore not analyzed in detail.

Another possible source of contamination is ascending fibers in the dorsolateral funiculus. However, this possibility appears unlikely as no spread of tracer to the dorsolateral funiculus was detected in any of our cases. Further, if ascending spinal fiber tracts had absorbed the tracer, we would have expected a certain amount of terminal labeling in the ipsilateral thalamus (34). We did not detect any such labeling in any of the cases.

The termination sites in the brainstem and thalamus

In agreement with previous studies on spinal and trigeminal projections in rat, cat and monkey (20, 23, 35-37), we found extensive anterograde labeling in the medial and lateral parts of PB, the CnF and the PAG following BDA injections into the ventrolateral C1/C2 dorsal horn. The

dominating thalamic targets following such injections were the Po, the PoT and the VPM (21, 22, 24). Anterograde labeling in the VPL was only evident when the tracer injections extended into laminae III-IV, and inputs to the VPL from this part of the spinal dorsal horn thus presumably originates in neurons in the deep dorsal horn laminae (cf. 24).

Several brainstem and thalamic nuclei likely to be important for the processing and modulation of nociceptive signals were devoid of anterograde labeling in our study. These include the nucleus of the solitary tract, the locus coeruleus and the raphe nuclei in the brainstem, and the intralaminar nuclei and the nucleus submedius (Sm) in the thalamus. Nor was any terminal labeling detected in any part of the hypothalamus. Except for Sm, all the above-mentioned nuclei or regions have been shown to receive projections from the cervical or medullary dorsal horns in different species (18, 20, 21, 24, 30). The absence of anterograde labeling in these nuclei in our experiments may be due to either an absence of such projections from this particular part of the dorsal horn, or that our small injections failed to label neurons with such projections. With respect to Sm, this nucleus appears to receive only sparse projections from the spinal dorsal horn in rats (18, 24), and trigeminal projections to Sm originate primarily from neurons in the rostral ventral part of the caudal spinal trigeminal nucleus (38). The absence of anterograde labeling in Sm in the present experiments is therefore not unexpected.

Functional significance: possible relation with headache

Which of the areas presently detected to contain anterograde labeling may serve a role in primary headache-related pain, and what is the particular role of each area? Considering that thin primary afferents from several cranial vessels terminate in laminae I-II (7-9) and that lamina I projection neurons serve a critical role in conducting nociceptive signals to higher centers (39), it appears likely that at least some of the brainstem and thalamic areas critical for

primary headaches are to be found among those anterogradely labeled following our BDA injections into laminae I-II. As ascending projections from the superficial dorsal horn originate almost exclusively from neurons in lamina I (e.g., 40), it appears most likely that the terminations we detected following our laminae I-II injections are from lamina I projection neurons. Below a number of the areas found to receive significant lamina I input from the lateral dorsal horn in segments C1 and C2 are discussed in further detail. However, it should be stressed that also the areas found to receive less abundant lamina I input and therefore not included in the sections below, may also serve important roles in primary headaches.

PAG. Accumulating evidence indicates that the PAG is able to inhibit and facilitate nociceptive responses. It receives input from nociceptive neurons in the spinal cord and sends projections to thalamic nuclei that process nociception (24, 36, 41, 42). The PAG is also a major component of a descending pain inhibitory system. Activation of this system inhibits nociceptive neurons in the dorsal horn of the spinal cord (for reviews, see 43, 44). It not only responds to somatic pain stimulation (e.g., 16) but also to cranial vasculature noxious stimulation (10-13). Animal experiments in rat, cat and monkey have shown that following electrical stimulation of the superior sagittal sinus or capsaicin injection into the cisterna magna, a dramatic increase in c-Fos expression is evident in the ventrolateral PAG (10, 12, 45). High-resolution fMRI demonstrate that patients with episodic migraine and chronic daily headache have an impaired iron homeostasis in the PAG during attacks, indicating a role of the PAG as a possible "generator" of migraine attacks (46). Our present finding of bilateral projections to the lateral/ventrolateral PAG from the C1/C2 superficial spinal dorsal horn, strongly support the assertion that the PAG is an important locus for the generation and/or modulation of pain in primary headaches.

PB. The PB, especially its lateral part, has long been recognized for its involvement in the processing of somatic and visceral noxious information in the CNS (47-51, for review, see

52). It receives abundant input from spinal and trigeminal lamina I neurons (35-37, 51) that are driven by Aδ- and/or C-fibers (51, 52). After application of capsaicin into the cisterna magna, c-Fos immunoreactivity is significantly increased in the PB (12). Together with our present data, this finding indicates important roles for the LPB in primary headaches, possibly including a function as a "relay" for nociceptive signals directed to the thalamus as well as to centers involved in homeostatic mechanisms (53).

CnF. A possible involvement of the CnF in the initiation of locomotion was recognized many years ago. Electrical stimulation of the CnF, and the adjacent pedunculopontine nucleus, induced controlled locomotion (54). Subsequently, a role more related with sympathetic vasomotor excitation was recognized for the CnF (55). Although a putative role in nociception was noticed two decades ago (e.g., 56, 57), it was not until more recently that such a function of the CnF was further substantiated (16, 17, 58, 59). In man, fMRI demonstrated significant activation in the CnF, the PAG and the PB, when visceral or somatic pain is induced by repeated electrical stimulation (16, 17, 59). Previous studies as well as our present findings support that the CnF receives afferent inputs from presumed nociceptive spinal and medullary lamina I dorsal horn neurons (20, 56, 60). The CnF also receives massive input from the PAG (61). The available evidence thus supports that the CnF is involved in mechanism associated with pain, including those related to headaches.

Po and PoT. The Po has in different species been shown to receive massive spinal and trigeminal projections from both superficial and deep dorsal horn neurons (18, 20, 22, 24, 62). Po neurons usually have large receptive field and are excited by more than one receptor type (63). The PoT is a caudal extention of Po, located between the medial portion of the medial geniculate nucleus and the APT. Gauriau and Bernard (64) showed that 45% of the PoT units are nociceptive specific, 19% are nociceptive non-specific, and 36% are tactile. They also demonstrated that PoT neurons convey nociceptive signals from lamina I and deep dorsal horn

neurons to the second somatosensory and insular cortices. As we presently observed that the input to PoT includes afferents from the craniovascular-receptive zone in the dorsal horn, sensory signals from cranial vessels, including nociceptive signals, might be relayed through the PoT towards cortical areas possibly involved some aspects of pain perception.

VPM. The VPM primarily relays sensory signals from the trigeminal system to the cerebral cortex. In rats, trigeminal projections to the VPM include those from the superficial laminae in the caudal spinal trigeminal nucleus (24). Considering the close relationship between the caudal spinal trigeminal nucleus and the rostralmost level of the spinal dorsal horn, it appears reasonable that lamina I input from the latter region may target the VPM rather than the VPL, as indicated by our present findings. Thus, also the VPM may serve as a thalamocortical relay for nociceptive signals originating in cranial blood vessels.

Acknowledgements

This project was supported by the Swedish Research Council (Project Nos. 5958 and 14276), and by AstraZeneca's Headache, Pfizer AB and GlaxoSmithKline's Migraine stipends.

References

1 Edvinsson L, Uddman R. Neurobiology in primary headaches. Brain Res Brain Res Rev 2005; 48:438-56.

2 Arbab MA, Wiklund L, Svendgaard NA. Origin and distribution of cerebral vascular innervation from superior cervical, trigeminal and spinal ganglia investigated with retrograde and anterograde WGA-HRP tracing in the rat. Neuroscience 1986; 19:695-708.

3 Arbab MA, Delgado T, Wiklund L, Svendgaard NA. Brain stem terminations of the trigeminal and upper spinal ganglia innervation of the cerebrovascular system: WGA-HRP transganglionic study. J Cereb Blood Flow Metab 1988; 8:54-63.

4 Goadsby PJ, Zagami AS. Stimulation of the superior sagittal sinus increases metabolic activity and blood flow in certain regions of the brainstem and upper cervical spinal cord of the cat. Brain 1991; 114:1001-11.

5 Goadsby PJ, Hoskin KL. The distribution of trigeminovascular afferents in the nonhuman primate brain Macaca nemestrina: a c-fos immunocytochemical study. J Anat 1997; 190:367-75.

6 Hoskin KL, Zagami AS, Goadsby PJ. Stimulation of the middle meningeal artery leads to Fos expression in the trigeminocervical nucleus: a comparative study of monkey and cat. J Anat 1999; 194:579-88.

7 Liu Y, Zhang M, Broman J, Edvinsson L. Central projections of sensory innervation of the rat superficial temporal artery. Brain Res 2003; 966:126-33.

8 Liu Y, Broman J, Edvinsson L. Central projections of sensory innervation of the rat superior sagittal sinus. Neuroscience 2004; 129:431-7.

9 Liu Y, Broman J, Edvinsson L. Central projections of sensory innervation of middle meningeal artery of rat. Brain Res 2008; 1208:103-10.

10 Keay KA, Bandler R. Vascular head pain selectively activates ventrolateral periaqueductal gray in the cat. Neurosci Lett 1998; 245:58-60.

11 Knight YE, Goadsby PJ. The periaqueductal grey matter modulates trigeminovascular input: a role in migraine? Neuroscience 2001; 106:793-800.

12 Ter Horst GJ, Meijler WJ, Korf J, Kemper RH. Trigeminal nociception-induced cerebral Fos expression in the conscious rat. Cephalalgia 2001; 21:963-75.

13 Knight YE, Classey JD, Lasalandra MP, Akerman S, Kowacs F, Hoskin KL, Goadsby PJ. Patterns of fos expression in the rostral medulla and caudal pons evoked by noxious craniovascular stimulation and periaqueductal gray stimulation in the cat. Brain Res 2005; 1045:1-11.

14 Weiller C, May A, Limmroth V, Juptner M, Kaube H, Schayck RV, et al. Brain stem activation in spontaneous human migraine attacks. Nat Med 1995; 1:658-60.

15 Bahra A, Matharu MS, Buchel C, Frackowiak RS, Goadsby PJ. Brainstem activation specific to migraine headache. Lancet 2001; 357:1016-7.

16 Dunckley P, Wise RG, Fairhurst M, Hobden P, Aziz Q, Chang L, Tracey I. A comparison of visceral and somatic pain processing in the human brainstem using functional magnetic resonance imaging. J Neurosci 2005; 25:7333-41.

17 Keltner JR, Furst A, Fan C, Redfern R, Inglis B, Fields HL. Isolating the modulatory effect of expectation on pain transmission: a functional magnetic resonance imaging study. J Neurosci 2006; 26:4437-43.

18 Cliffer KD, Burstein R, Giesler GJ Jr. Distributions of spinothalamic, spinohypothalamic, and spinotelencephalic fibers revealed by anterograde transport of PHA-L in rats. J Neurosci 1991; 11:852-68.

19 Iwata K, Kenshalo DR Jr, Dubner R, Nahin RL. Diencephalic projections from the superficial and deep laminae of the medullary dorsal horn in the rat. J Comp Neurol 1992; 321:404-20.

20 Craig AD. Distribution of brainstem projections from spinal lamina I neurons in the cat and the monkey. J Comp Neurol 1995; 361:225-48.

21 Craig AD. Distribution of trigeminothalamic and spinothalamic lamina I terminations in the cat. Somatosens Mot Res 2003; 20:209-22.

22 Craig AD. Distribution of trigeminothalamic and spinothalamic lamina I terminations in the macaque monkey. J Comp Neurol 2004; 477:119-48.

23 Potts JT, Lee SM, Anguelov PI. Tracing of projection neurons from the cervical dorsal horn to the medulla with the anterograde tracer biotinylated dextran amine. Auton Neurosci 2002; 98:64-9.

24 Gauriau C, Bernard JF. A comparative reappraisal of projections from the superficial laminae of the dorsal horn in the rat: the forebrain. J Comp Neurol 2004; 468:24-56.

25 Paxinos G, Watson C. The Rat Brain in Stereotaxic Coordinates, 3rd edn. Sydney: Academic Press. 1997.

26 Schmued L, Kyriakidis K, Heimer L. In vivo anterograde and retrograde axonal transport of the fluorescent rhodamine-dextran-amine, Fluoro-Ruby, within the CNS. Brain Res 1990; 526:127-34.

27 Zhang M, Broman J. Cervicothalamic tract termination: a reexamination and comparison with the distribution of monoclonal antibody Cat-301 immunoreactivity in the cat. Anat Embryol (Berl) 1998; 198:451-72.

28 Wouterlood FG, Jorritsma-Byham B. The anterograde neuroanatomical tracer biotinylated dextran-amine: comparison with the tracer Phaseolus vulgaris-leucoagglutinin in preparations for electron microscopy. J Neurosci Methods 1993; 48:75-87.

29 Browne PA, Clark GT, Kuboki T, Adachi NY. Concurrent cervical and craniofacial pain. A review of empiric and basic science evidence. Oral Surg Oral Med Oral Pathol Oral Radiol Endod 1998; 86:633-40.

30 Malick A, Strassman RM, Burstein R. Trigeminohypothalamic and reticulohypothalamic tract neurons in the upper cervical spinal cord and caudal medulla of the rat. J Neurophysiol 2000; 84:2078-112.

31 Zhang M, Liu Y, Broman J. Organization of the ferret lateral cervical nucleus and cervicothalamic tract. Somatosens Motor Res 2002; 19:36-48.

32 Mouton LJ, Klop E-M, Broman J, Zhang M, Holstege G. Lateral cervical nucleus projections to periaqueductal gray matter in the cat. J Comp Neurol 2004; 471:434-45.

33 Giesler GJ Jr, Bjorkeland M, Xu Q, Grant G. Organization of the spinocervicothalamic pathway in the rat. J Comp Neurol 1988; 268:223-33.

34 Stevens RT, Apkarian AV, Hodge CJ Jr. The location of spinothalamic axons within spinal cord white matter in cat and squirrel monkey. Somatosens Mot Res 1991; 8:97-102

35 Slugg RM, Light AR. Spinal cord and trigeminal projections to the pontine parabrachial region in the rat as demonstrated with Phaseolus vulgaris leucoagglutinin. J Comp Neurol 1994; 339:49-61.

36 Bernard JF, Dallel R, Raboisson P, Villanueva L, Le Bars D. Organization of the efferent projections from the spinal cervical enlargement to the parabrachial area and periaqueductal gray: a PHA-L study in the rat. J Comp Neurol 1995; 353:480-505.

37 Li J, Xiong K, Pang Y, Dong Y, Kaneko T, Mizuno N. Medullary dorsal horn neurons providing axons to both the parabrachial nucleus and thalamus. J Comp Neurol 2006; 498:539-51.

38 Yoshida A, Dostrovsky JO, Sessle BJ, Chiang CY. Trigeminal projections to the nucleus submedius of the thalamus in the rat. J Comp Neurol 1991; 307:609-25.

39 Craig AD. Pain mechanisms: Labeled lines versus convergence in central processing. Annu Rev Neurosci 2003; 26:1-30.

40 Burstein R, Dado RJ, Giesler GJ Jr. The cells of origin of the spinothalamic tract of the rat: a quantitative reexamination. Brain Res 1990; 511:329-37.

41 Mantyh PW. Connections of midbrain periaqueductal gray in the monkey. I. Ascending efferent projections. J Neurophysiol 1983; 49:567-81.

42 Keay KA, Bandler R. Anatomical evidence for segregated input from the upper cervical spinal cord to functionally distinct regions of the periaqueductal gray region of the cat. Neurosci Lett 1992; 139:143-8.

43 Behbehani MM. Functional characteristics of the midbrain periaqueductal gray. Prog Neurobiol 1995; 46:575-605.

44 Vanegas H, Schaible HG. Descending control of persistent pain: inhibitory or facilitatory? Brain Res Brain Res Rev 2004; 46:295-309.

45 Hoskin KL, Bulmer DC, Lasalandra M, Jonkman A, Goadsby PJ. Fos expression in the midbrain periaqueductal grey after trigeminovascular stimulation. J Anat 2001; 198:29-35.

46 Welch KM, Nagesh V, Aurora SK, Gelman N. Periaqueductal gray matter dysfunction in migraine: cause or the burden of illness? Headache 2001; 41:629-37.

47 Bernard JF, Besson JM. The spino(trigemino)pontoamygdaloid pathway: electrophysiological evidence for an involvement in pain processes. J Neurophysiol 1990; 63:473-90.

48 Bernard JF, Huang GF, Besson JM. The parabrachial area: electrophysiological evidence for an involvement in visceral nociceptive processes. J Neurophysiol 1994; 71:1646-60.

49 Bester H, Menendez L, Besson JM, Bernard JF. Spino (trigemino) parabrachiohypothalamic pathway: electrophysiological evidence for an involvement in pain processes. J Neurophysiol 1995; 73:568-85.

50 Bester H, Matsumoto N, Besson JM, Bernard JF. Further evidence for the involvement of the spinoparabrachial pathway in nociceptive processes: a c-Fos study in the rat. J Comp Neurol 1997; 383:439-58.

51 Bester H, Chapman V, Besson JM, Bernard JF. Physiological properties of the lamina I spinoparabrachial neurons in the rat. J Neurophysiol 2000; 83:2239-59.

52 Gauriau C, Bernard JF. Pain pathways and parabrachial circuits in the rat. Exp Physiol 2002; 87:251-8.

53 Craig AD. Interoception: The sense of the physiological condition of the body. Curr Op Neurobiol 2003; 13:500-5.

54 Skinner RD, Garcia-Rill E. The mesencephalic locomotor region (MLR) in the rat. Brain Res 1984; 323:385-9.

55 Verberne AJ. Cuneiform nucleus stimulation produces activation of medullary sympathoexcitatory neurons in rats. Am J Physiol. 1995; 268:R752-8.

56 Hylden JL, Hayashi H, Dubner R, Bennett GJ. Physiology and morphology of the lamina I spinomesencephalic projection. J Comp Neurol 1986; 247:505-15.

57 Zemlan FP, Behbehani MM. Nucleus cuneiformis and pain modulation: anatomy and behavioral pharmacology. Brain Res 1988; 453:89-102.

58 Carlson JD, Iacono RP, Maeda G. Nociceptive excited and inhibited neurons within the pedunculopontine tegmental nucleus and cuneiform nucleus. Brain Res 2004; 1013:182-7.

59 Zambreanu L, Wise RG, Brooks JC, Iannetti GD, Tracey I. A role for the brainstem in central sensitisation in humans. Evidence from functional magnetic resonance imaging. Pain 2005; 114:397-407.

60 Wiberg M, Westman J, Blomqvist A. Somatosensory projection to the mesencephalon: an anatomical study in the monkey. J Comp Neurol 1987; 264:92-117.

61 Mantyh PW. Connections of midbrain periaqueductal gray in the monkey. II. Descending efferent projections. J Neurophysiol 1983; 49:582-94.

62 Craig AD, Burton H. The distribution and topographical organization in the thalamus of anterogradely-transported horseradish peroxidase after spinal injections in cat and raccoon. Exp Brain Res 1985; 58:227-54.

63 Albe-Fessard D, Berkley KJ, Kruger L, Ralston HJ 3rd, Willis WD Jr. Diencephalic mechanisms of pain sensation. Brain Res 1985; 356:217-96.

64 Gauriau C, Bernard JF. Posterior triangular thalamic neurons convey nociceptive messages to the secondary somatosensory and insular cortices in the rat. J Neurosci 2004; 24:752-61.

Figure legends

Figure 1 Drawings and photomicrographs depicting the BDA injection sites in the different cases. (A) Schematic drawing showing the injection sites for all 9 rats on a longitudinal plane from C3 to Sp5C dorsal horn (laminae I-V). The shaded background in laminae I-IV depicting the putative sensory nerve termination area with an arbitrary density gradient from investigated cranial blood vessels based on our previous works (7-9). (B), (C) and (D) Schematic drawings of the injection sites on transverse plane in laminae I-II (B; rats 26, 56 and 58), laminae I-IV (C; rats 51, 55, 85 and 87) and laminae I-IV with extension into the LCN (D; rats 27 and 29). (E) and (F) Examples of injection sites in the ventrolateral dorsal horn, either limited to laminae I-II in rostral C1 (E; rat 26) or laminae I-IV in rostral C2 (F; rat 85). Scale bar = 200 in (F) (valid for E and F).

Figure 2 Plots of the distributions of labeled terminations in the pons, the midbrain and the thalamus in two individual cases after a BDA injection into laminae I-II (A; rat 26) or laminae I-IV (B; rat 85). BDA was injected into the right side of the spinal dorsal horn. In the pons and midbrain, anterograde labeling was observed both ipsilaterally and contralaterally, while in the thalamus terminal labeling was only observed contralaterally. Note the more extensive labeling (including, e.g., the SG and the VPL) in rat 85 than in rat 26. Scale bar = 1mm. For abbreviations, see the List of *abbreviations*.

Figure 3 Photomicrographs showing anterograde BDA labeling in the pons and the midbrain after a BDA injection into laminae I-II of rat 26. (A1), (B1), (C1) and (D1) show the cytoarchitecture of the selected brainstem sections (thionin staining). (A2), (B2), (C2) and (D2) are from the adjacent BDA-labeled sections and show the areas corresponding to those

indicated by rectangles in (A1), (B1), (C1) and (D1). Scale bar = 500 μm in (D1) (valid for A1, B1, C1 and D1). Scale bar = 50 μm in (D2) (valid for A2, B2, C2 and D2).

Figure 4 Photomicrographs showing anterograde BDA labeling in the thalamus. (A1), (B1) (from rat 26) and (C1) (from rat 85) are from thionin-stained sections. (A2), (B2) and (C2) (from adjacent sections) show BDA labeled terminals in the PoT, the VPM and the VPL in the areas corresponding to the rectangles in (A1), (B1) and (C1), respectively. Scale bar = 500 μm in (C1) (valid for A1, B1 and C1). Scale bar = 50 μm in (C2) (valid for A2, B2 and C2).

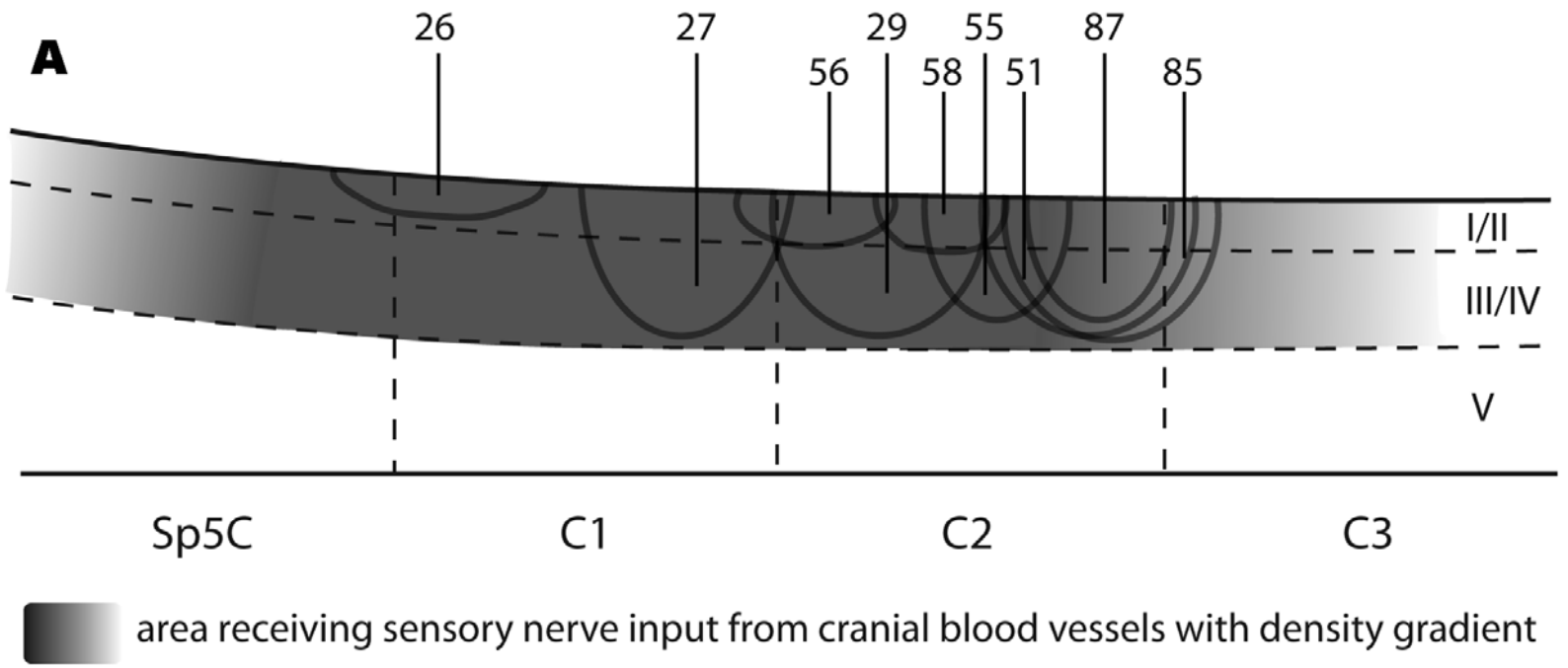

area receiving sensory nerve input from cranial blood vessels with density gradient

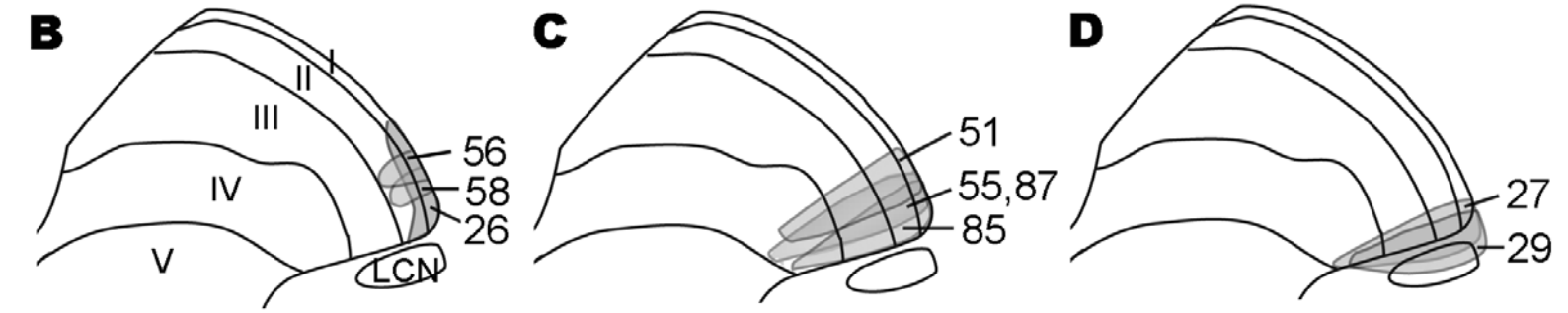

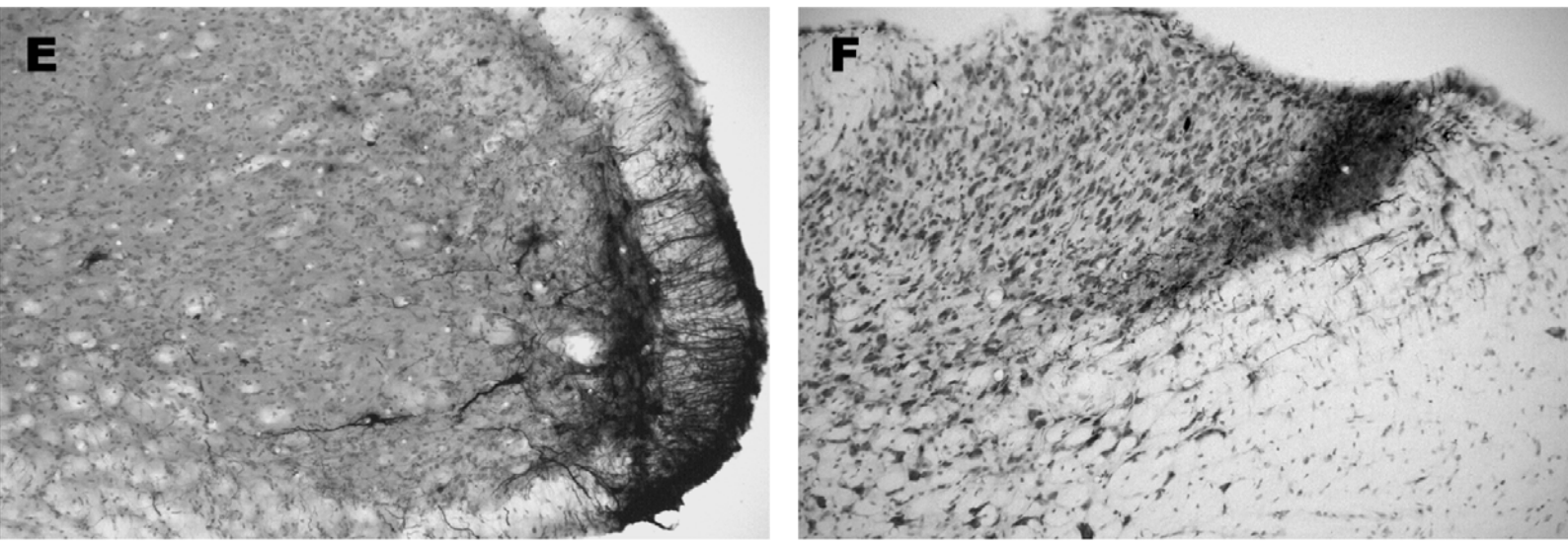

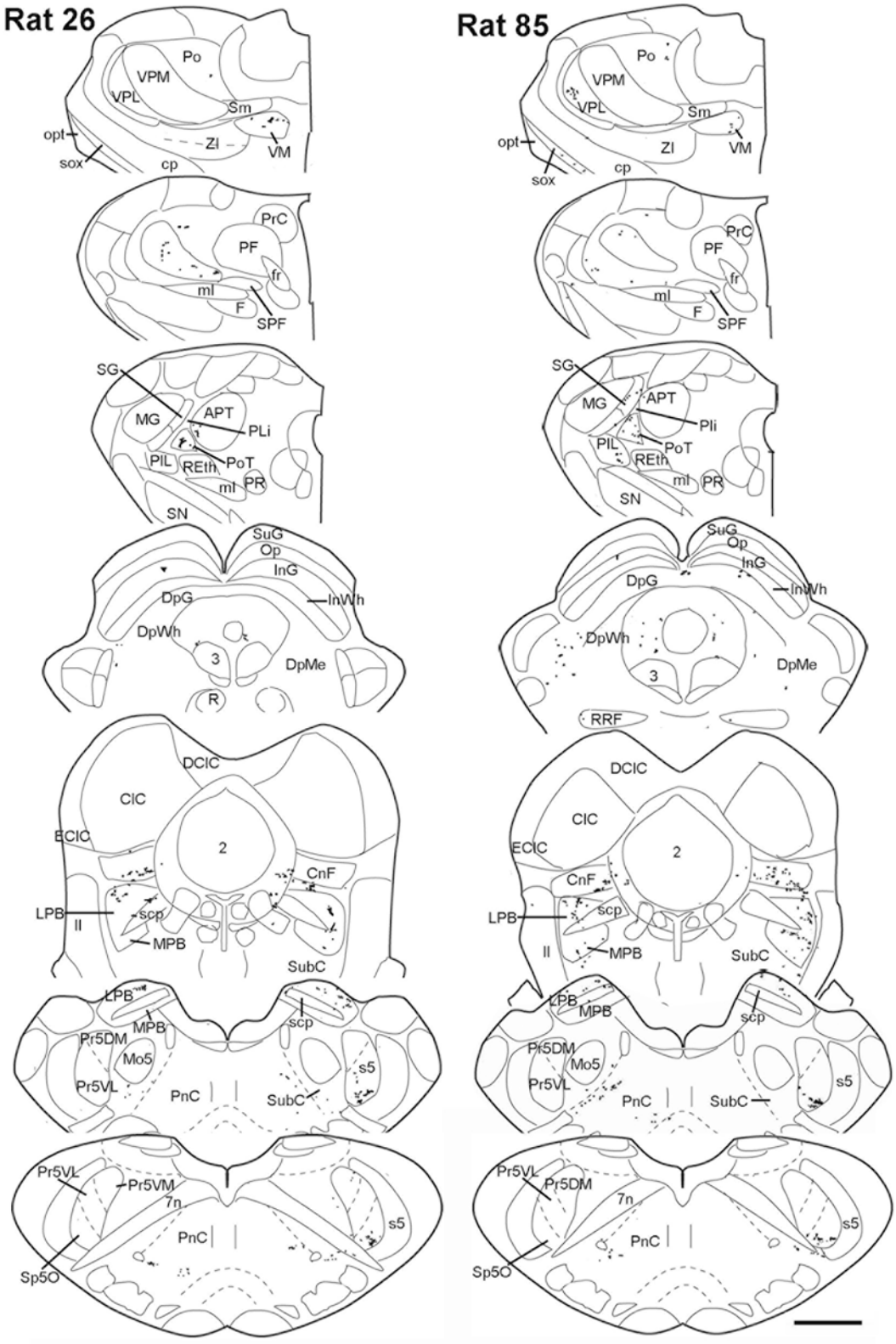
Rat 26
Po
VPM
VPL
Sm
opt
ZI
VM
sox
cp
PrC
PF
fr
ml
F
SPF
SG
MG
APT
PLi
PIL
REth
PoT
ml
PR
SN
SuG
Op
InG
DpG
InWh
DpWh
3
DpMe
R
DCIC
CIC
ECIC
2
CnF
LPB
II
scp
MPB
SubC
LPB
MPB
scp
Pr5DM
Mo5
s5
Pr5VL
PnC
SubC
Pr5VL
Pr5VM
7n
s5
PnC
Sp5O
Rat 85
Po
VPM
VPL
Sm
opt
ZI
VM
sox
cp
PrC
PF
fr
ml
F
SPF
SG
MG
APT
Pli
PIL
PoT
REth
ml
PR
SN
SuG
Op
InG
DpG
InWh
DpWh
3
DpMe
RRF
DCIC
CIC
ECIC
2
CnF
LPB
scp
II
MPB
SubC
LPB
MPB
scp
Pr5DM
Mo5
s5
Pr5VL
PnC
SubC
Pr5VL
Pr5DM
7n
s5
PnC
Sp5O

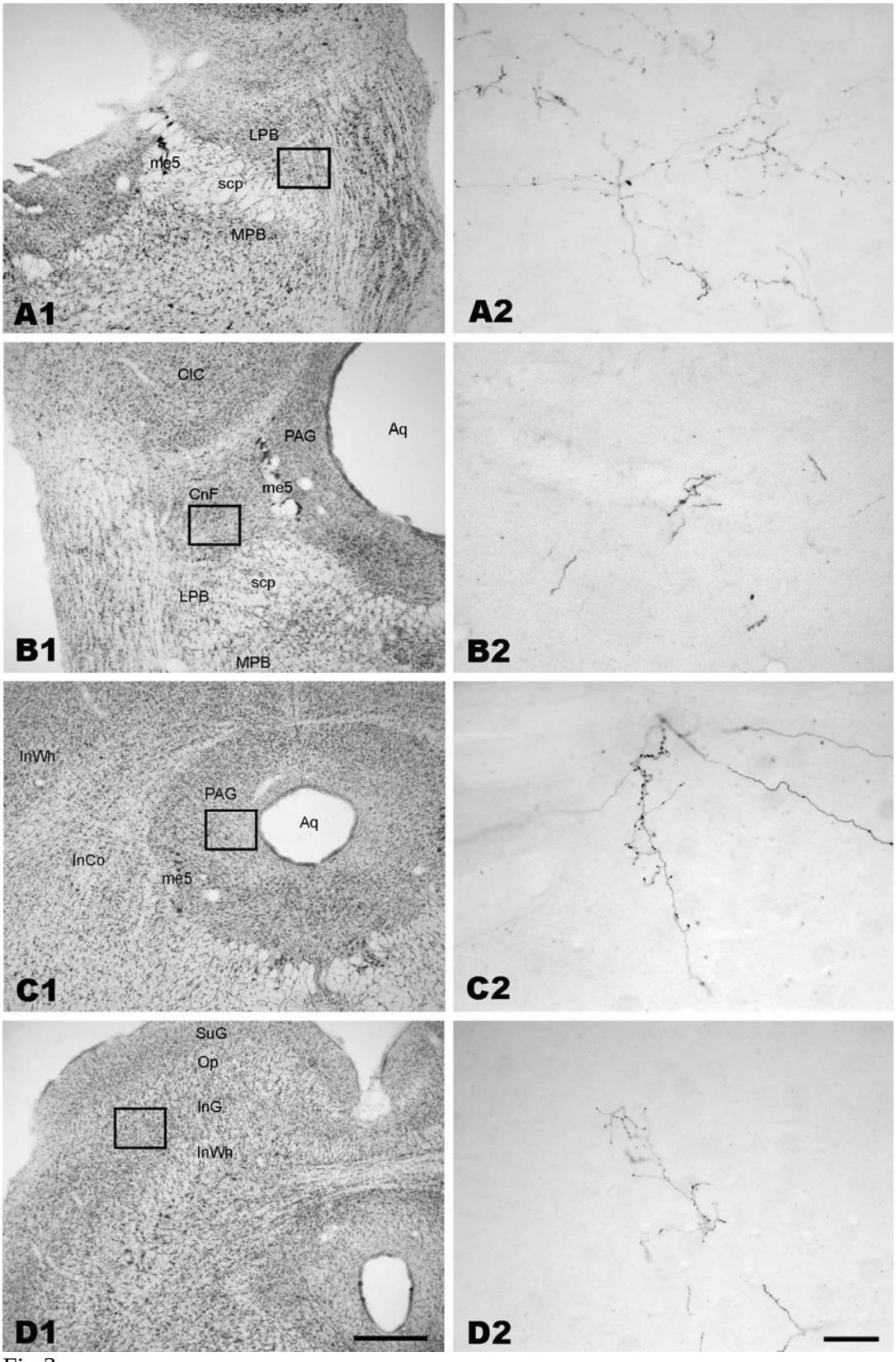
LPB
me5
scp
MPB
A1
A2
CIC
PAG
Aq
CnF
me5
scp
LPB
MPB
B1
B2
InVh
PAG
Aq
InCo
me5
C1
C2
SuG
Op
InG
InVh
D1
D2

Fig 3

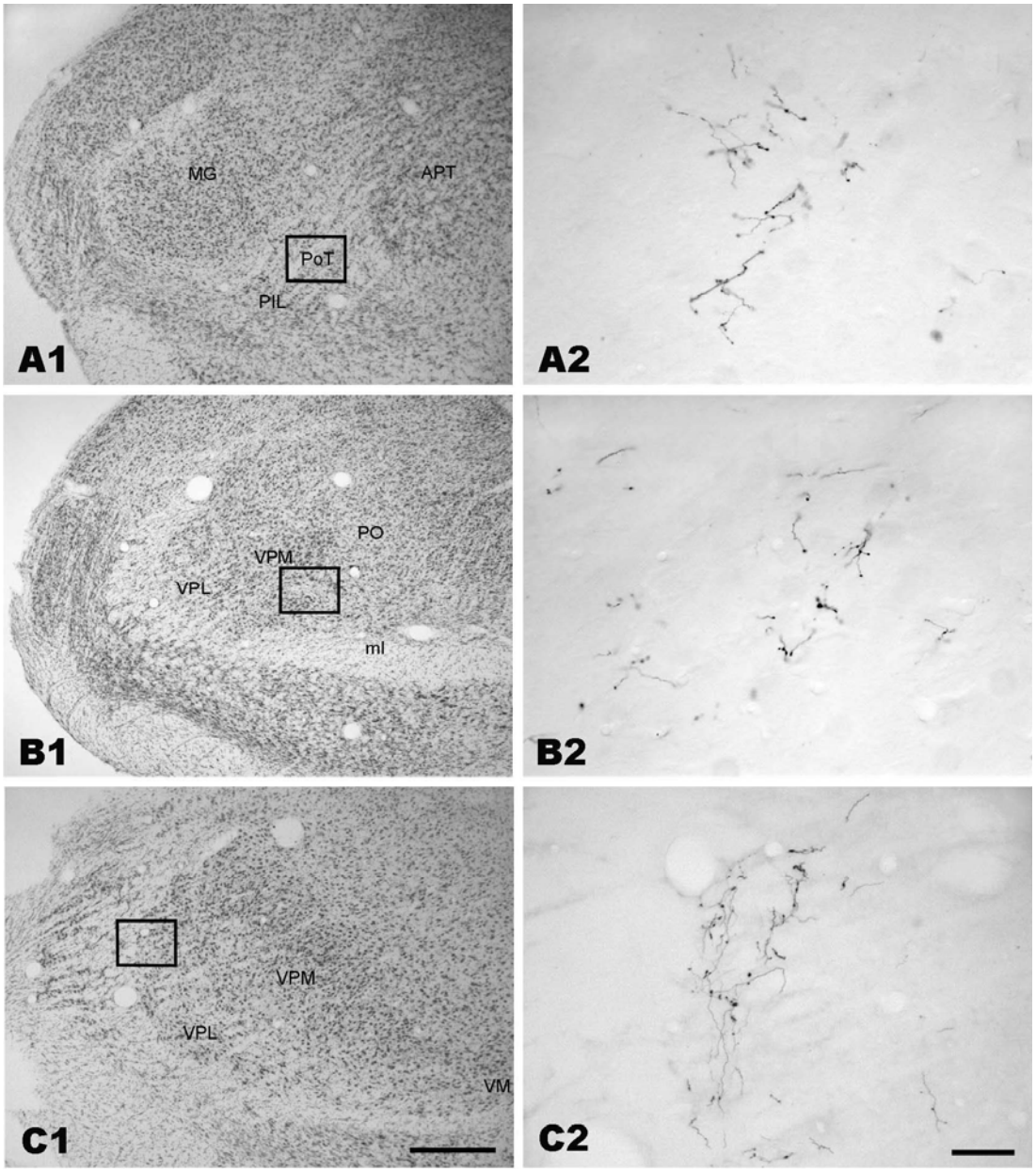

Fig 4

Table 1 Locations and density of BDA-labeled varicosities in the pons, the midbrain and the thalamus from all analyzed rats

Animal number	**Rat 26**	**Rat 56**	**Rat 58**	**Rat 51**	**Rat 55**	**Rat 85**	**Rat 87**	**Rat 27**	**Rat 29**
Injection sites (segment/laminae)	C1/I-II	C2/I-II	C2/I-II	C2/I-IV	C2/I-IV	C2/I-IV	C2/I-IV	C2/I-IV, LCN	C2/I-IV, LCN
Pons									
SubC	+ ¤				++ ¤¤	+ ¤¤	++ ¤¤	+	+ ¤
PnC	++ ¤¤	++ ¤	+ ¤	++ ¤	+ ¤	++	+ ¤	+ ¤	+ ¤¤
LPB	+++¤¤¤	++ ¤¤	++ ¤	++	+++¤¤¤	+++¤¤¤	+++¤¤¤	+++¤¤¤	++ ¤¤
MPB	+ ¤	+ ¤	¤		+ ¤	++ ¤¤¤	+ ¤	++ ¤	+ ¤
Midbrain									
Cnf	++ ¤	++	+ ¤	++	++	++ ¤¤	+	++ ¤¤	+
DpMe	++	++	++	+	++	++ ¤	++	++ ¤¤	+ ¤
PAG	++ ¤¤¤	++ ¤¤	+++ ¤	+		++ ¤¤	+++ ¤¤	+++ ¤¤	++
CIC								+++	+++
ECIC								+	++
InG	++ ¤¤	++			++	+ + ¤¤	++	++ ¤	+++
DpG						+ ¤	+		+
APT	++		++	++	+	++	+	+	++
Thalamus									
SG				++		++	++	++	++
PoT	+++	++	+++	+++	++	+++	+++	++	++
Po	++					+	++	+++	++
PIL				+++	+	+++	++	++	+
VPM	+++		++			++	++	+++	++
VPL						+++	+++	+++	+++
VM	++					++			

1. +, contralateral labeling; ¤, ipsilateral labeling.
2. Density of terminal fibers: + / ¤, sparse; ++ / ¤¤, moderate; +++ / ¤¤¤, dense.
3. For abbreviations, see list.